DETC2021-67819

CONFORMAL TOPOLOGY OPTIMIZATION OF HEAT CONDUCTION PROBLEMS ON MANIFOLDS USING AN EXTENDED LEVEL SET METHOD (X-LSM)

Xiaoqiang Xu[1]
[1]Department of Mechanical Engineering
State University of New York at Stony Brook
Stony Brook, NY 11794, USA
Email:Xiaoqiang.Xu@stonybrook.edu

Shikui Chen[1,*]
[1]Department of Mechanical Engineering
State University of New York at Stony Brook
Stony Brook, NY 11794, USA
Email: shikui.chen@stonybrook.edu

Xianfeng David Gu[2,3]
[2]Department of Computer Science
[3]Department of Applied Mathematics & Statistics
State University of New York at Stony Brook,
Stony Brook, NY 11794, USA
Email: gu@cs.stonybrook.edu

Michael Yu Wang[4]
[4]Department of Mechanical and Aerospace Engineering
Hong Kong University of Science and Technology
Clear Water Bay, Kowloon, Hong Kong
Email: mywang@ust.hk

ABSTRACT

In this paper, the authors propose a new dimension reduction method for level-set-based topology optimization of conforming thermal structures on free-form surfaces. Both the Hamilton-Jacobi equation and the Laplace equation, which are the two governing PDEs for boundary evolution and thermal conduction, are transformed from the 3D manifold to the 2D rectangular domain using conformal parameterization. The new method can significantly simplify the computation of topology optimization on a manifold without loss of accuracy. This is achieved due to the fact that the covariant derivatives on the manifold can be represented by the Euclidean gradient operators multiplied by a scalar with the conformal mapping. The original governing equations defined on the 3D manifold can now be properly modified and solved on a 2D domain. The objective function, constraint, and velocity field are also equivalently computed with the FEA on the 2D parameter domain with the properly modified form. In this sense, we are solving a 3D topology optimization problem equivalently on the 2D parameter domain. This reduction in dimension can greatly reduce the computing cost and complexity of the algorithm. The proposed concept is proved through two examples of heat conduction on manifolds.

Keywords

Heat conduction. Conformal topology optimization. Conformal mapping. Conformal invariance. Laplace equation. Extended level set method.

1 INTRODUCTION

Efficient thermal management is essential to many engineering applications to maintain a moderate temperature field and extend the lifespan of the devices. Topology optimization, which seeks to find the optimum material distributions of the design for the desired performance, has been a powerful tool for the conceptual design of thermal structures in recent years [1–5]. In particular, extensive studies have been conducted on the topology optimization of heat conduction problems [6–11]. For instance,

---

*Address all correspondence to this author.

1

Iga et al. [12] carried out topology optimization of thermal conductors considering the design-dependent effects using the homogenization method. Gersborg-Hansen et al. [13] used the solid isotropic material with penalization (SIMP) based topology optimization method and the finite volume method (FVM) to solve a 2D thermal conduction problem. Qing et al. [14] applied the evolutionary structural optimization (ESO) to efficiently reduce the temperature at selected control points. Zhuang et al. [15] tackled the problem of level-set-based topology optimization on heat conduction under multiple load cases. Xia et al. [16] revisited the heat conduction topology optimization problems by combining the level set method with the bidirectional evolutionary optimization (BESO) method to achieve better hole nucleation flexibility. Yamada et al. [17] investigated a thermal diffusivity maximization problem with generic heat transfer boundaries under the level set framework, where a fictitious interface energy was incorporated to regulate the topology optimization problem.

Among the different methods of topology optimization [18–22], the level set methods [21,22] are getting attention because of its clear boundary expression and flexibility in handling topological changes. The aforementioned level-set-based topology optimizations of heat conduction problems mainly deal with 2D planar cases. But in practice, heat conductors as free-form surfaces may have broader applications than 2D planar designs [23, 24]. The extended level set method (X-LSM) proposed by Chen and Gu et al. [25] systematically investigated the structural shape and topology optimization on manifolds by integrating the conformal geometry theory [26, 27] into the level set framework. The key ingredient of the X-LSM is to conformally map the original manifold to a 2D rectangular domain where the modified Hamilton-Jacobi equation is solved to evolve the structural boundaries. The rationality behind this modification lies in that the corresponding covariant derivatives on a surface can be represented by the Euclidean differential operators multiplied by a scaling factor based on the conformal parameterization [28]. This method elegantly extends the conventional level-set-based topology optimizations from the Euclidean space to manifolds.

In the conventional X-LSM, only the Hamilton-Jacobi equation, which governs the boundary evolution, is transferred from the original manifold to the mapped 2D domain. However, the finite element analysis (FEA) is always conducted on the original free-form surfaces. The FEA costs the majority of the computing time in topology optimization [29]. In this paper, in order to further reduce the computing cost and algorithm complexity, we conduct the FEA on the mapped 2D domain. We essentially reduce the dimension of FEA by equivalently transforming the Laplace equation from the 3D surface to the 2D planar domain. It reduces the total number of degrees of freedom (DOF), and thus results in the reduction of the overall computational cost. Beside, the FEA implementation can also be simplified by moving the FEA from the 3D surface to the 2D rectangular domain where the mesh generation can be much easier than

the original manifold. Similar to the derivation of the modified Hamilton-Jacobi equation in the conventional X-LSM, we need to derive the corresponding modified thermal conduction equations on the 2D mapped domain to ensure consistency with the FEA performed on the original 3D manifold. As for the heat conduction problems studied in this paper, the governing equation is the Laplace equation with no body heat source. One of the characteristics of the Laplace equation is its conformal invariance. That is, the conformal mapping does not change the solution to the Laplace equation on the original manifold and its corresponding 2D plane [30]. In other words, we can equally solve the Laplace equation on the 2D mapped domain without losing accuracy. Usually, the three quantities, namely, the objective function, the current volume, and the velocity field, are computed on the 3D manifold together with the FEA. In this paper, we transfer the FEA from the manifold to the 2D parameter domain equivalently. The three quantities will also be evaluated from the FEA on the 2D domain with a properly modified form to ensure consistency. Several numerical examples are presented to demonstrate the effectiveness of the proposed methodology.

This paper is organized as follows: Section 2 will provide some theoretical background, including the conventional level set method, the conformal mapping theory and X-LSM, the Laplace equation and its conformal invariance. The problem formulation will be detailed in Section 3, followed by the numerical implementation in Section 4. Numerical examples and discussions will be presented in Section 5. Section 6 will conclude with some closing remarks.

2 THEORETICAL BACKGROUND

This section will provide theoretical background underlying the formulation of the proposed method.

2.1 Conventional Level Set Method

Initiated by Allaire [22] and Wang [21], level set method has become a promising shape and topology optimization method, particularly for multimaterial and multiphysics problems. Level set method could generate and maintain a clear boundary during the optimization process, with the structural boundary implicitly represented as the zero contour of a one-higher dimensional level set function. It is a preferred property when a detailed description of the boundary is required. In the classical level set framework, the level set function is defined on a fixed background grid. The structural design is implicitly embedded in the level set function $\Phi(\mathbf{x}, t)$ as follows:

$$\begin{cases} \Phi(\mathbf{x},t) > 0, & x \in \Omega, & \text{material} \\ \Phi(\mathbf{x},t) = 0, & x \in \partial\Omega, & \text{boundary} \\ \Phi(\mathbf{x},t) < 0, & x \in D/\Omega, & \text{void} \end{cases} \quad (1)$$

The geometric level set model for a 2D structural boundary is shown in Figure 1. For the structural boundary, it always sat-
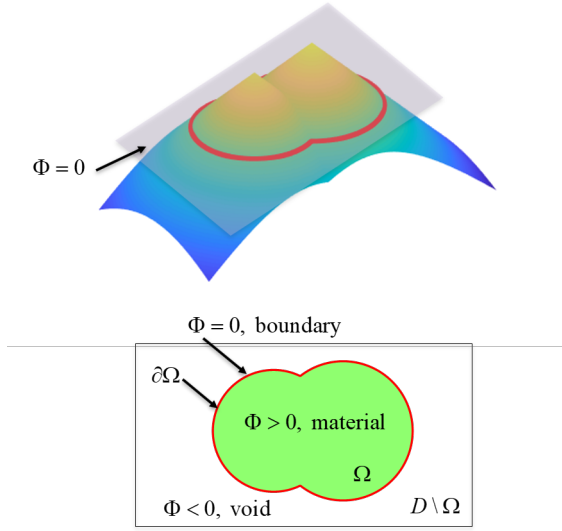
FIGURE 1. THE LEVEL SET REPRESENTATION OF A 2D DE-SIGN

isfies the equation $\Phi(\mathbf{x},t) = 0$. By differentiating both sides of the equation with respect to a pseudo time t, we could obtain the Hamilton-Jacobi (H-J) equation [31]:

$$\frac{\partial \Phi(\mathbf{x},t)}{\partial t} - V_n \cdot |\nabla\Phi| = 0, \quad (2)$$

where $V_n = V \cdot (-\frac{\nabla\Phi}{|\nabla\Phi|}) = \frac{d\mathbf{x}}{dt} \cdot (-\frac{\nabla\Phi}{|\nabla\Phi|})$. The dynamics of the structural boundary evolution is governed by the above H-J equation. The shape sensitivity analysis can be conducted using the adjoint sensitivity method. The design velocity field is constructed from case to case depending on the specific optimization problems at hand.

2.2 Conformal Mapping Theory and Extended Level Set Method (X-LSM)

A conformal mapping is essentially a function that locally preserves angles, but not necessarily lengths. It originates from differential geometry on the Riemannian manifold [26]. A visualization of the angle preservation property of conformal mapping is shown in Figure 2, where the infinitesimal circles are mapped to infinitesimal circles from the 3D surface to the 2D disk. The conformal mapping theory has found many applications in the fields of engineering. Our particular interest is its application to solving PDEs on manifolds [27, 28]. With the conformal parameterization, the differential operators defined on the manifolds can be transferred into its Euclidean forms with a combination of the conformal factor $e^{2\lambda}$ describing the scaling effect of the conformal mapping. Specifically, let M be a mani-
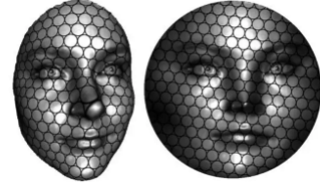

FIGURE 2. CONFORMAL MAPPING FROM 3D SURFACE TO 2D DISK [26]

fold and $\phi : \mathbb{R}^2 \to M$ be a global conformal parameterization of M. Suppose the conformal factor of ϕ is $e^{2\lambda}$. A scalar function is defined on the manifold as $f : M \to \mathbb{R}$. Then the gradient of f on the manifold can be represented as:

$$\begin{aligned} \nabla_M f &= \partial_x f \mathbf{i} + \partial_y f \mathbf{j} \\ &= e^{-\lambda} \frac{\partial f \circ \phi}{\partial x} \mathbf{i} + e^{-\lambda} \frac{\partial f \circ \phi}{\partial y} \mathbf{j}, \end{aligned} \quad (3)$$

where $\mathbf{i} = e^{-\lambda}\frac{\partial}{\partial x}$, $\mathbf{j} = e^{-\lambda}\frac{\partial}{\partial y}$. For the detailed derivations, the interested readers are referred to [27, 28].

Resting on this fact, the conventional Hamilton-Jacobi equation on the manifold can be rewritten as the modified H-J equation on the 2D parameter domain as follows [25]:

$$\frac{\partial \Phi(\mathbf{x},t)}{\partial t} - e^{-\lambda} V_n \cdot |\nabla\Phi| = 0. \quad (4)$$

In this way, the boundary evolution initially on the 3D manifold can now be realized by solving the modified H-J equation on the 2D domain, which reduces the complexity of the calculation.

2.3 Conformal Invariance of the Laplace Equation

Based on our earlier work of the modified H-J equation, we try to advance the current X-LSM by transferring the FEA also to the mapped 2D domain. To this end, we need to derive the corresponding governing equations on the 2D rectangular domain. For the heat conduction problems, the governing equation is the Laplace equation where there is no body heat source. One characteristic of the Laplace equation is its conformal invariance, which means the equation takes the same form under the conformal parameterization. A brief derivation for the plane to plane conformal mapping cases can be readily given as follows with the aid of complex analysis.

Consider the real valued function $U(\xi, \eta)$ and the analytic map $w = f(z) = f(x+iy) = \xi(x,y) + i\eta(x,y)$, where ξ and η are real valued functions. If $U(\xi, \eta)$ is a harmonic function of ξ and η, then the composition $u(x,y) = U(\xi(x,y), \eta(x,y))$ is also a harmonic function of x, y. To prove it, we first apply the chain rule as below:

$$\frac{\partial u}{\partial x} = \frac{\partial U}{\partial \xi}\frac{\partial \xi}{\partial x} + \frac{\partial U}{\partial \eta}\frac{\partial \eta}{\partial x}, \frac{\partial u}{\partial y} = \frac{\partial U}{\partial \xi}\frac{\partial \xi}{\partial y} + \frac{\partial U}{\partial \eta}\frac{\partial \eta}{\partial y}. \quad (5)$$

$$\frac{\partial^2 u}{\partial x^2} = \frac{\partial^2 U}{\partial \xi^2}(\frac{\partial \xi}{\partial x})^2 + 2\frac{\partial^2 U}{\partial \xi \partial \eta}\frac{\partial \xi}{\partial x}\frac{\partial \eta}{\partial x} + \frac{\partial^2 U}{\partial \eta^2}(\frac{\partial \eta}{\partial x})^2 \\ + \frac{\partial U}{\partial \xi}\frac{\partial^2 \xi}{\partial x^2} + \frac{\partial U}{\partial \eta}\frac{\partial^2 \eta}{\partial x^2}. \quad (6)$$

$$\frac{\partial^2 u}{\partial y^2} = \frac{\partial^2 U}{\partial \xi^2}(\frac{\partial \xi}{\partial y})^2 + 2\frac{\partial^2 U}{\partial \xi \partial \eta}\frac{\partial \xi}{\partial y}\frac{\partial \eta}{\partial y} + \frac{\partial^2 U}{\partial \eta^2}(\frac{\partial \eta}{\partial y})^2 \\ + \frac{\partial U}{\partial \xi}\frac{\partial^2 \xi}{\partial y^2} + \frac{\partial U}{\partial \eta}\frac{\partial^2 \eta}{\partial y^2}. \quad (7)$$

Then the conformal mapping on 2D satisfies the Cauchy-Riemann equation:

$$\frac{\partial \xi}{\partial x} = -\frac{\partial \eta}{\partial y}, \frac{\partial \xi}{\partial y} = \frac{\partial \eta}{\partial x}. \quad (8)$$

After some algebra, we will arrive at:

$$\Delta u = \frac{\partial^2 u}{\partial x^2} + \frac{\partial^2 u}{\partial y^2} = [(\frac{\partial \xi}{\partial x})^2 + (\frac{\partial \eta}{\partial x})^2](\frac{\partial^2 U}{\partial \xi^2} + \frac{\partial^2 U}{\partial \eta^2}) = |f'(z)|^2 \Delta U. \quad (9)$$

This equation implies that if u is harmonic in a region of the z-plane, U is also harmonic in a conformally mapped region of the w-plane.

3 CONFORMAL TOPOLOGY OPTIMIZATION OF HEAT CONDUCTION PROBLEMS ON MANIFOLDS

3.1 Problem Formulation

In this study, we consider a steady-state heat conduction problem. All the material properties are assumed to be isotropic. The governing equations for the heat conduction phenomena are as follows:
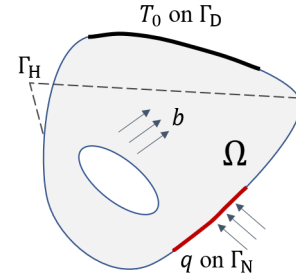

FIGURE 3. DIAGRAM OF A HEAT CONDUCTOR

$$-k\nabla^2 T = b, \; in \; \Omega \\ k\nabla T \cdot \mathbf{n} = q, \; on \; \Gamma_N \\ k\nabla T \cdot \mathbf{n} = 0, \; on \; \Gamma_H \\ T = T_0, \; on \; \Gamma_D \quad (10)$$

where k is the thermal conductivity; T is the state variable temperature; b is the rate of internal heat generation; n is the outward unit normal vector of the structural boundary; q is the heat flux in the inward normal direction. As shown in Figure 3, the structural boundaries are composed of a Dirichlet boundary Γ_D with $T = T_0$, a homogeneous Neumann boundary Γ_H which is adiabatic, and a non-homogeneous Neumann boundary Γ_N with a heat flux q. It is noted that when there is no body heat source,

<div align="center">4</div>

that is, $b = 0$, the heat equation is reduced to the Laplace equation, which holds the property of conformal invariance.

The weak form of the heat equations can be obtained by first multiplying a test function $\bar{T}$, integrating over the whole domain, utilizing the product rule, and applying the 2D divergence theorem with the above-mentioned boundary conditions. The weak form of the governing equation is as follows:

$$a(T, \bar{T}) = l(\bar{T}), \ \forall \bar{T} \in U_{ad} \tag{11}$$

where $\bar{T}$ is the test function for the temperature and U_{ad} is the space of the virtual temperature field satisfying the same boundary conditions. The bilinear function on the left side of equation (11) is defined as

$$a(T, \bar{T}) = \int_{\Omega} k \nabla T \cdot \nabla \bar{T} d\Omega. \tag{12}$$

The linear function on the right side of equation (11) is defined as

$$l(\bar{T}) = \int_{\Omega} b \bar{T} d\Omega + \int_{\Gamma_N} q \bar{T} ds. \tag{13}$$

The objective of the optimization problems is to minimize the thermal compliance under a volume constraint, which is set as follows:

$$\begin{aligned}
&\underset{\Omega}{Inf} \ \ J = \int_{\Omega} b T d\Omega + \int_{\Gamma_N} q T ds, \\
&S.t. \ \ a(T, \bar{T}) = l(\bar{T}), \ \forall \bar{T} \in U_{ad} \\
&\qquad V(\Omega) = V^*,
\end{aligned} \tag{14}$$

where $V(\Omega) = \int_{\Omega} dx$ denotes the volume of the design, and V^* is the target volume.

3.2 Shape Sensitivity Analysis

To evolve the structural boundaries by solving the Hamilton-Jocabi equation under the level set framework, the shape derivatives need to be conducted to provide a proper normal velocity field that can drive the boundary propagation

toward the next better design [21, 22]. In this study, the material derivative method [32] and the adjoint method [33] are employed for the shape derivatives. The Lagrangian of the optimization problem is defined as

$$L = J(T) + a(T, \bar{T}) - l(\bar{T}). \tag{15}$$

The material derivative of the Lagrangian is given:

$$\frac{DL}{Dt} = \frac{DJ(T)}{Dt} + \frac{Da(T, \bar{T})}{Dt} - \frac{Dl(\bar{T})}{Dt}. \tag{16}$$

The material derivative of the objective function $J(T)$ is:

$$\begin{aligned}
\frac{DJ(T)}{Dt} = &\int_{\Omega} (b'T + bT') d\Omega + \int_{\Gamma} bTV_n ds \\
&+ \int_{\Gamma} (q'T + qT') ds + \int_{\Gamma} (\frac{\partial(qT)}{\partial \mathbf{n}} + k_c qT) \cdot V_n ds.
\end{aligned} \tag{17}$$

The material derivative of the weak-form governing equation is:

$$\begin{aligned}
\frac{Da(T, \bar{T})}{Dt} - \frac{Dl(\bar{T})}{Dt} = &\int_{\Omega} k[\nabla T' \cdot \nabla \bar{T} + \nabla T \cdot \nabla \bar{T}'] d\Omega \\
&+ \int_{\Gamma} k \nabla T \cdot \nabla \bar{T} \cdot V_n ds - \int_{\Omega} (b'\bar{T} + b\bar{T}') d\Omega - \int_{\Gamma} b\bar{T} \cdot V_n ds \\
&- \int_{\Gamma} (q'\bar{T} + q\bar{T}') ds - \int_{\Gamma} (\frac{\partial(q\bar{T})}{\partial \mathbf{n}} + k_c q\bar{T}) \cdot V_n ds.
\end{aligned} \tag{18}$$

Collecting all the terms containing $\bar{T}'$ as follows:

$$\int_{\Omega} k \nabla T \cdot \nabla \bar{T}' d\Omega - \int_{\Omega} b\bar{T}' d\Omega - \int_{\Gamma} q\bar{T}' ds = 0. \tag{19}$$

we recover the weak form of the state equation as $a(T, \bar{T}') = l(\bar{T}')$, for $\forall \bar{T}' \in U_{ad}$. Suppose the b and q are not time-dependent, and q is a nodal flux, the material derivatives for the Lagrangian can be rewritten as:

5

$$\frac{DL}{Dt} = \int_\Omega bT'd\Omega + \int_\Gamma bTV_n ds + \int_\Gamma qT'ds$$
$$+ \int_\Omega k[\nabla T' \cdot \nabla \bar{T}]d\Omega + \int_\Gamma k\nabla T \cdot \nabla \bar{T} \cdot V_n ds \qquad (20)$$
$$- \int_\Gamma b\bar{T} \cdot V_n ds.$$

Collecting the terms containing T' and making the sum equal to zero, we can obtain the adjoint equation:

$$\int_\Omega bT'd\Omega + \int_\Gamma qT'ds + \int_\Omega k[\nabla T' \cdot \nabla \bar{T}]d\Omega = 0. \qquad (21)$$

We can readily solve out the adjoint variable $\bar{T} = -T$. The remaining part for the material derivatives of the Lagrangian reads:

$$\frac{DL}{Dt} = \int_\Gamma bTV_n ds + \int_\Gamma k\nabla T \cdot \nabla \bar{T} \cdot V_n ds$$
$$- \int_\Gamma b\bar{T} \cdot V_n ds. \qquad (22)$$

Substituting $\bar{T} = -T$ into the above equation and applying the steepest descent method, the design velocity field can be constructed as:

$$V_{n1} = -2bT + k\nabla T \cdot \nabla T. \qquad (23)$$

For the volume constraint, the augmented Lagrangian method [32, 34] is employed. The augmented objective function will be given as:

$$\hat{J} = J + \varphi(\Omega) = J + \lambda(V(\Omega) - V^*) + \frac{1}{2\mu}(V(\Omega) - V^*)^2, \quad (24)$$

where λ is the Lagrangian multiplier, and μ is a penalty parameter set by the designer and is close to zero. During the optimization process, the update schemes for λ and μ are as follows:

$$\lambda^{k+1} = \max\{0, \lambda^k + \frac{1}{\mu^k}(V(\Omega) - V^*)\},$$
$$\mu^{k+1} = \alpha \cdot \mu^k, \qquad (25)$$

where $\alpha \in (0,1)$. After conducting the material derivative of $\varphi(\Omega)$ and applying the steepest descent method, the velocity field responsible for the volume constraint can be given as:

$$V_{n2} = -(\lambda + \frac{1}{\mu}(V(\Omega) - V^*)). \qquad (26)$$

Finally, the normal velocity field that drives the boundary evolution can be given as:

$$V_n = V_{n1} + V_{n2} = -2bT + k\nabla T \cdot \nabla T - (\lambda + \frac{1}{\mu}(V(\Omega) - V^*)). \qquad (27)$$

4 NUMERICAL IMPLEMENTATION
4.1 Boundary Conditions of the 2D Parameter Domain

Figure 4 shows the workflow of the proposed method. The first step is to conformally map the 3D manifold to a rectangular parameter domain, where the level set function is initialized to give the initial design. The modified governing equation is still the Laplace equation due to its conformal invariance after conformal mapping. One thing that needs extra attention is the correspondences of the boundary conditions from the 3D manifold to the 2D parameter domain. As shown in Figure 3 and equation (10), the whole structural boundary consists of a Dirichlet boundary Γ_D with $T = T_0$, a homogeneous Neumann boundary Γ_H and a non-homogeneous Neumann boundary Γ_N. For the Dirichlet boundary, we assign the same T_0 to the corresponding mapped boundary on the 2D parameter domain since the scalar field T does not change its value under the conformal mapping. As for the Neumann boundary conditions, we need to modify the heat flux q based on Section 2.2. To be specific, the original non-homogeneous Neumann boundary condition is given as:

$$k\nabla_M T \cdot \mathbf{n} = q, \; on \; \Gamma_N \qquad (28)$$

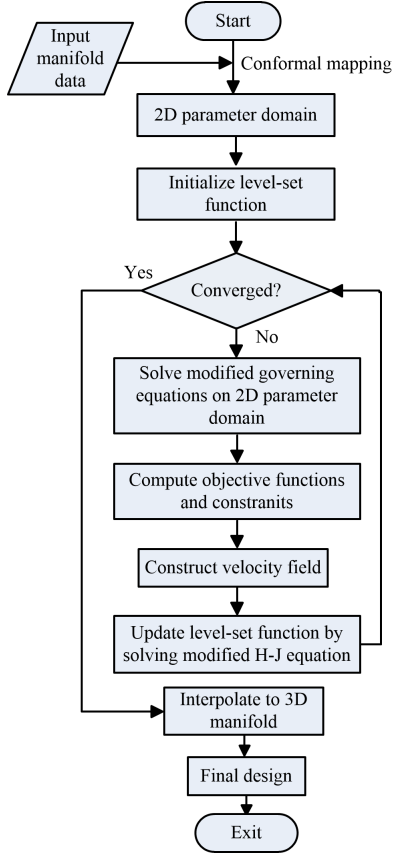Under the conformal parameterization, it should be rewritten as follows:

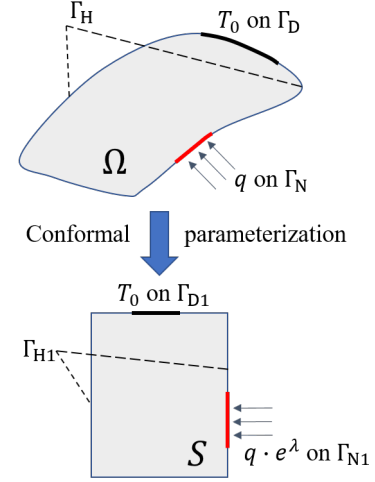**FIGURE 4**. THE FLOWCHART OF THE METHOD

$$ke^{-\lambda}\nabla T \cdot \mathbf{n}_1 = q, \; on \; \Gamma_{N1} \qquad (29)$$

where $\mathbf{n}_1$ is the normal vector of the boundary on the 2D parameter domain and Γ_{N1} corresponds to the non-homogeneous boundary on the 2D domain. From the above relation, we can have that the heat flux should be modified as $q \cdot e^\lambda$ on the 2D parameter domain. Physically, this makes sense in that the integral of the heat flux along the non-homogeneous Neumann boundary actually gives the power, which can be seen as the energy source into the system. Due to the scaling effect of the conformal parameterization, the length of the non-homogeneous Neumann boundary on the manifold differs a factor of e^λ from that on the 2D parameter domain. Assuming the 3D manifold and the 2D parameter domain share the same thickness, then the heat flux on the 2D domain can be approximately given as $q \cdot r$, where r is the ratio between the length of the non-homogeneous Neumann boundary on the 3D manifold and the 2D parameter domain. An illustration of the boundary correspondences is shown in Figure 5, assuming there is no body heat source.

FIGURE 5. THE BOUNDARY CONDITION CORRESPONDENCES

4.2 Evaluate Objective Function, Current Volume and Velocity Field Equivalently on 2D Parameter Domain

In a typical implementation of level-set-based topology optimization, the objective function, the current volume, and the velocity field are usually evaluated where the FEA is conducted. In this study, since the FEA is transferred onto the 2D parameter domain, we want to compute the above three quantities equivalently on the 2D domain. On the original 3D manifold, the expressions for the objective function, current volume and normal speed are respectively given as follows:

$$
\begin{aligned}
J &= \int_\Omega k\nabla_M T \cdot \nabla_M T d\Omega, \\
V &= \int_\Omega d\Omega, \\
V_{nT} &= k\nabla_M T \cdot \nabla_M T,
\end{aligned}
\qquad (30)
$$

where V_{nT} is the normal velocity component directly pertaining to the Lagrangian L (see equation (27)). Under the conformal parameterization, the above formulas should be properly modified as below according to Section 2.2:

$$
\begin{aligned}
J &= \int_S k\nabla T \cdot \nabla T dS, \\
V &= \int_S e^{2\lambda} dS, \\
V_{nT} &= ke^{-2\lambda}\nabla T \cdot \nabla T.
\end{aligned}
\qquad (31)
$$

In this way, the objective function, current volume, and the normal velocity field can now be equivalently evaluated on the 2D parameter domain.

5 NUMERICAL EXAMPLES

Two numerical examples are provided, and some comparisons with the results obtained by the conventional X-LSM are given to illustrate the effectiveness of the proposed method. For the two examples, all the dimension sizes are given in meters. The thermal conductivity for the solid material is given as $k = 10W/(m*K)$. To avoid singularity, an ersatz material model is employed with $k = 0.001W/(m*K)$ for the weak material.

5.1 A Fan-shaped Surface

The first numerical example is a fan-shaped surface as the 3D manifold shown in Figure 6 with the boundary conditions. A Dirichlet boundary condition $T = 0$ is assigned to the top and bottom curve segments in blue color. A heat flux $q = 10W/m^2$ is applied at the two side curve segments represented in red. The adiabatic thermal boundary condition is applied to other edges. These four curve segments in color sit in the middle with the length set as $1/10$ of the respective boundary edge lengths. The overall size of the manifold is $1 \times 1 \times 0.866$. The thickness of the shell model is uniform and set to be 0.01m. The volume ratio target is set as $V_f = 0.5$.
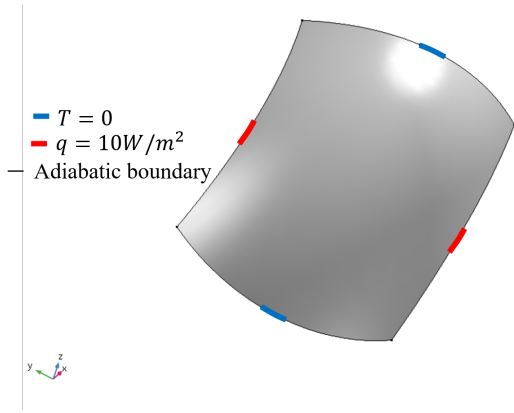

FIGURE 6. THE BOUNDARY CONDITION OF A FAN-SHAPED SURFACE

The plots of the initial design on the 2D parameter domain and the 3D manifold are given in Figure 7. The original manifold is meshed with 8644 triangular elements in the conventional X-LSM. The 2D parameter domain is a 0.8596×1 rectangle, which is meshed with 23370 triangular elements. On the 2D domain, there are 30 uniformly distributed holes to be the initial

design. According to subsection 4.1, the heat flux on the non-homogeneous Neumann boundary of the 2D parameter domain is set to be $q \cdot r = 10 \times 1.098 = 10.98\ W/m^2$. The final optimized
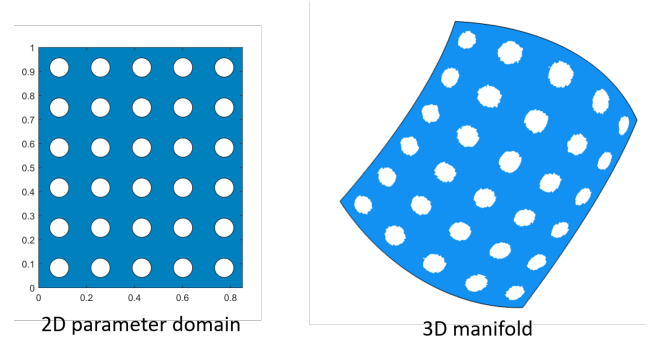

FIGURE 7. INITIAL DESIGN FOR THE FAN-SHAPED SURFACE

designs on the 2D parameter domain and the original fan-shaped manifold are given in Figures 8 and 9. We can notice that there is little difference in terms of topology between the results obtained using the proposed method and the conventional X-LSM where the FEA is still performed on the 3D manifold. Besides, the results are consistent with a 2D version heat conduction topology optimization result with similar boundary conditions [17]. The convergence history plots are given in Figure 10. The volume constraint $V_f = 0.5$ is satisfied for both methods. It is appealing that the objective function values are 0.61665 and 0.61057, respectively, for our proposal and the conventional X-LSM, which demonstrates the equivalence of conducting FEA on the 2D parameter domain.
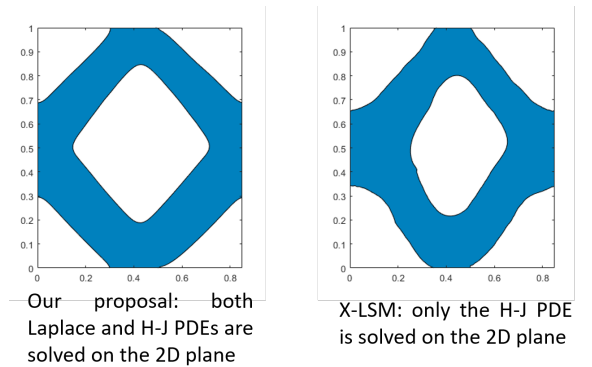

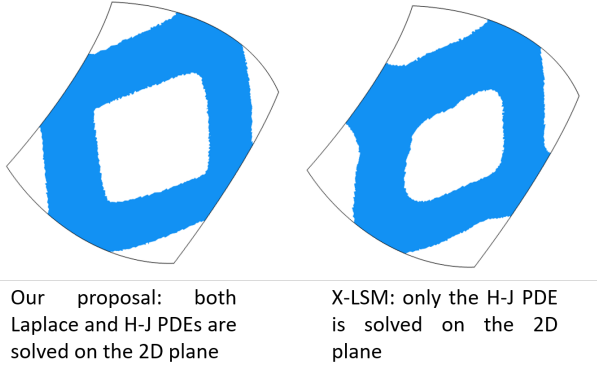
FIGURE 8. FINAL DESIGN ON THE 2D PARAMETER DOMAIN

Our proposal: both Laplace and H-J PDEs are solved on the 2D plane

X-LSM: only the H-J PDE is solved on the 2D plane

FIGURE 9. FINAL DESIGN ON THE FAN-SHAPED MANIFOLD

5.2 A Schwarz' P TPMS

The second numerical example is a Schwarz' P triply periodic minimal surface (TPMS). One interesting geometrical feature of a TPMS is its large surface area, which is suitable for applications like chemical reactions or heat and mass transfer [35]. A TPMS can be approximated by a level set equation. Taking the Schwarz' P surface as an example, the approximation can be given as:

$$\phi_P \equiv cos\, x + cos\, y + cos\, z = c, \qquad (32)$$

where c is a constant. A Schwarz' P surface is shown in Figure 11. Due to the symmetry, we select a quarter of Schwarz' P TPMS for simplicity. The boundary conditions are shown in Figure 12. A Dirichlet boundary condition $T = 0$ is assigned to the top edge in blue. A heat flux $q = 10W/m^2$ is applied at the bottom edge represented in red. All other boundaries are adiabatic. The overall size of the Schwarz' P TPMS unit is 6.2×6.2×6.2. For the quarter unit cell, the overall size is 3.1×3.1×6.2. The thickness is uniform and set to be 0.01m. The volume ratio target is set to $V_f = 0.7$.

The plots of the initial design on the 2D parameter domain and the 3D manifold are given in Figure 13. The original manifold is meshed with 25032 triangular elements in the conventional X-LSM. The 2D parameter domain is a 0.5687 × 1 rectangle, which is meshed with 19726 triangular elements. On the 2D parameter domain, there are 20 uniformly distributed holes in the initial design. Based on subsection 4.1, the heat flux on the non-homogeneous Neumann boundary of the 2D parameter domain is set to be $q \cdot r = 10×4.224$=42.24 W/m^2.

The final designs optimized on the 2D parameter domain and the original quarter Schwarz' P TPMS are shown in Figures 14 and 15. The results obtained by the proposed method and by the conventional X-LSM are almost identical. Figure 16 shows the
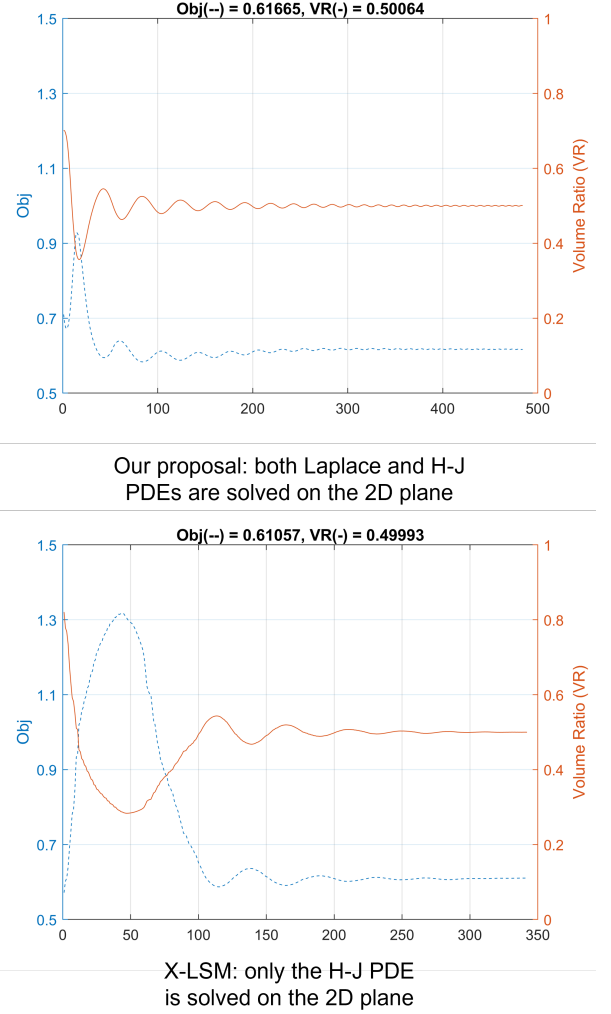

Our proposal: both Laplace and H-J PDEs are solved on the 2D plane

X-LSM: only the H-J PDE is solved on the 2D plane

FIGURE 10. CONVERGENCE HISTORY OF THE FAN-SHAPED SURFACE EXAMPLE

convergence history plots. The volume constraint is satisfied for both methods. The final objective function values are 190.48 and 196.47, respectively, for our proposal and the conventional X-LSM. The discrepancy of the objective function value is within the acceptable range. The final optimized design on the Schwarz' P TPMS unit is shown in Figure 17. In Figure 18, a 3×3 assembled Schwarz' P TPMS array is constructed with the optimized unit cell using the proposed method. Such a device may be used in a heat exchanger.

6 CONCLUSIONS AND FUTURE WORK

This paper proposes a new dimension reduction method for topology optimization of conformal thermal structures on freeform surfaces. The original 3D topology optimization problems
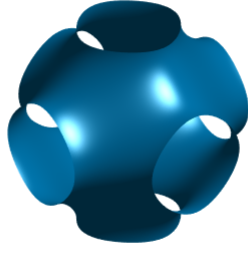
FIGURE 13. INITIAL DESIGN FOR THE QUARTER SCHWARZ' P SURFACE

FIGURE 11. A SCHWARZ' P SURFACE

$T = 0$
$q = 10W/m^2$
Adiabatic boundary

Our proposal: both Laplace and H-J PDEs are solved on the 2D plane

X-LSM: only the H-J PDE is solved on the 2D plane
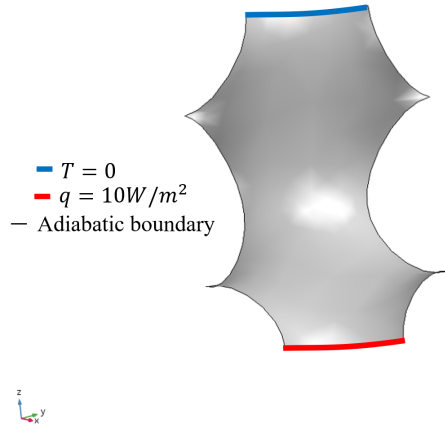
FIGURE 14. FINAL DESIGN ON THE 2D PARAMETER DOMAIN

FIGURE 12. THE BOUNDARY CONDITION OF A QUARTER SCHWARZ' P SURFACE

defined on manifolds can now be equivalently solved on the 2D parameter domain with the incorporation of conformal geometry theory. Both the Hamilton-Jacobi equation and the governing equation are transferred to the 2D rectangular domain. This is achieved due to the fact that the covariant derivatives on the manifold can be represented by the Euclidean gradient operators multiplied by a scalar under the conformal parameterization. The physical quantities necessary for the optimization process are also evaluated equivalently on the 2D parameter domain.

In this study, a heat conduction topology optimization problem on the 3D manifold is addressed using the proposed methodology. When there is no body heat source, the governing equation is essentially the Laplace equation, which is invariant through conformal mapping. Two numerical examples are provided and some comparisons with the conventional X-LSM are given to demonstrate the effectiveness of the proposed method. The objective function, i.e., thermal compliance, design volume, and
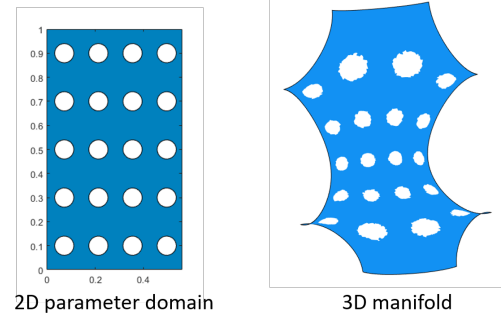
the velocity field, is computed equivalently on the 2D parameter domain with a properly modified form. Good agreement is achieved between the optimized designs using our proposal and the conventional X-LSM.

Although the proposed method can significantly reduce the computational cost and algorithm complexity due to its dimension reduction, the main focus of this paper is to demonstrate the feasibility of the methodology. In future work, the performance of the proposed method in terms of saving computational cost will be systematically investigated. One thing that needs to be mentioned is that the proposed method can be easily applied to topology optimization problems where the governing equation is in the form of Laplace equation, e.g., electric conduction and electrostatics problems. For such physics, the conformal invariance can be directly utilized. Specifically, the modified governing equation on the 2D parameter domain will remain as a Laplace equation but with different boundary conditions. The extension of the proposed methodology to other topology optimization problems with different physics equations, e.g., Poisson's equation, will also be our next research focus.
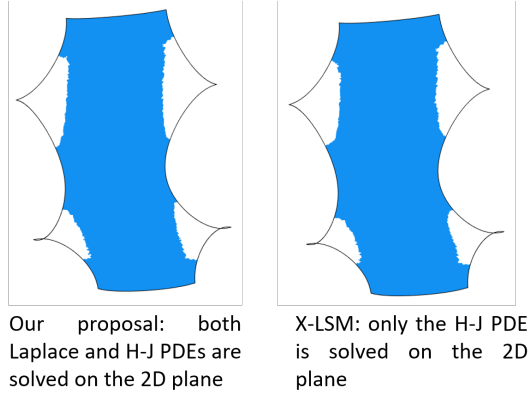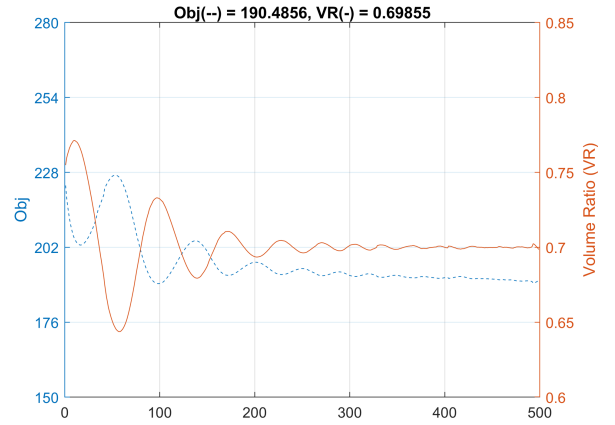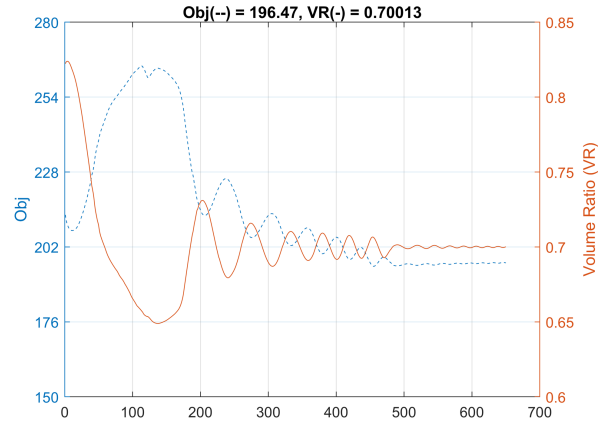
FIGURE 15. FINAL DESIGN ON THE QUARTER SCHWARZ' P SURFACE

ACKNOWLEDGMENT

Our proposal: both Laplace and H-J PDEs are solved on the 2D plane

X-LSM: only the H-J PDE is solved on the 2D plane

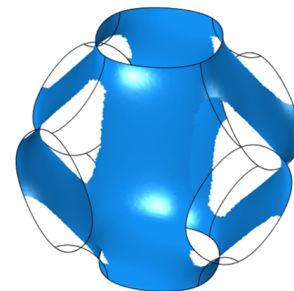**FIGURE 16**. CONVERGENCE HISTORY OF QUARTER SCHWARZ' P SURFACE EXAMPLE

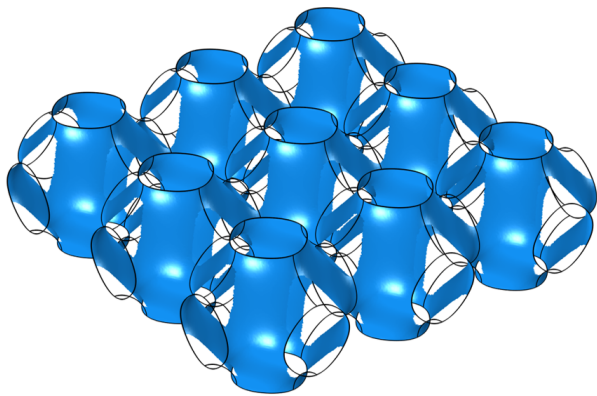**FIGURE 17**. FINAL DESIGN ON A SCHWARZ' P TPMS UNIT

FIGURE 18.   3×3 ASSEMBLED SCHWARZ' P TPMS ARRAY

REFERENCES

[1] Dbouk, T., 2017. "A review about the engineering design of optimal heat transfer systems using topology optimization". *Applied Thermal Engineering, 112*, pp. 841–854.

[2] Dede, E. M., 2009. "Multiphysics topology optimization of heat transfer and fluid flow systems". In proceedings of the COMSOL Users Conference.

[3] Sun, S., Liebersbach, P., and Qian, X., 2020. "3d topology optimization of heat sinks for liquid cooling". *Applied Thermal Engineering, 178*, p. 115540.

[4] Lei, T., Alexandersen, J., Lazarov, B. S., Wang, F., Haertel, J. H., De Angelis, S., Sanna, S., Sigmund, O., and Engelbrecht, K., 2018. "Investment casting and experimental testing of heat sinks designed by topology optimization". *International Journal of Heat and Mass Transfer, 127*, pp. 396–412.

[5] Alexandersen, J., Sigmund, O., and Aage, N., 2016. "Large scale three-dimensional topology optimisation of heat sinks cooled by natural convection". *International Journal of Heat and Mass Transfer, 100*, pp. 876–891.

[6] Donoso, A., and Pedregal, P., 2005. "Optimal design of 2d conducting graded materials by minimizing quadratic functionals in the field". *Structural and Multidisciplinary Optimization, 30*(5), pp. 360–367.

[7] Burger, F. H., Dirker, J., and Meyer, J. P., 2013. "Three-dimensional conductive heat transfer topology optimisation in a cubic domain for the volume-to-surface problem". *International Journal of Heat and Mass Transfer, 67*, pp. 214–224.

[8] Zhang, Y., Qiao, H., and Liu, S., 2011. *Design of the heat conduction structure based on the topology optimization*. INTECH Open Access Publisher.

[9] Bruns, T. E., 2007. "Topology optimization of convection-dominated, steady-state heat transfer problems". *International Journal of Heat and Mass Transfer, 50*(15-16), pp. 2859–2873.

[10] Zhu, B., Zhang, X., Wang, N., and Fatikow, S., 2016. "Optimize heat conduction problem using level set method with a weighting based velocity constructing scheme". *International Journal of Heat and Mass Transfer, 99*, pp. 441–451.

[11] Lazarov, B. S., Alexandersen, J., and Sigmund, O., 2014. "Topology optimized designs of steady state conduction heat transfer problems with convection boundary conditions". *EngOpt*.

[12] Iga, A., Nishiwaki, S., Izui, K., and Yoshimura, M., 2009. "Topology optimization for thermal conductors considering design-dependent effects, including heat conduction and convection". *International Journal of Heat and Mass Transfer, 52*(11-12), pp. 2721–2732.

[13] Gersborg-Hansen, A., Bendsøe, M. P., and Sigmund, O., 2006. "Topology optimization of heat conduction problems using the finite volume method". *Structural and multidisciplinary optimization, 31*(4), pp. 251–259.

[14] Li, Q., Steven, G. P., Xie, Y. M., and Querin, O. M., 2004. "Evolutionary topology optimization for temperature reduction of heat conducting fields". *International Journal of Heat and Mass Transfer, 47*(23), pp. 5071–5083.

[15] Zhuang, C., Xiong, Z., and Ding, H., 2007. "A level set method for topology optimization of heat conduction problem under multiple load cases". *Computer methods in applied mechanics and engineering, 196*(4-6), pp. 1074–1084.

[16] Xia, Q., Shi, T., and Xia, L., 2018. "Topology optimization for heat conduction by combining level set method and beso method". *International Journal of Heat and Mass Transfer, 127*, pp. 200–209.

[17] Yamada, T., Izui, K., and Nishiwaki, S., 2011. "A level set-based topology optimization method for maximizing thermal diffusivity in problems including design-dependent effects". *Journal of Mechanical Design, 133*(3).

[18] Bendsøe, M. P., and Kikuchi, N., 1988. "Generating optimal topologies in structural design using a homogenization method". *Computer methods in applied mechanics and engineering, 71*(2), pp. 197–224.

[19] Bendsøe, M. P., 1989. "Optimal shape design as a material distribution problem". *Structural optimization, 1*(4), pp. 193–202.

[20] Xie, Y. M., and Steven, G. P., 1993. "A simple evolutionary procedure for structural optimization". *Computers & structures, 49*(5), pp. 885–896.

[21] Wang, M. Y., Wang, X., and Guo, D., 2003. "A level set method for structural topology optimization". *Computer methods in applied mechanics and engineering, 192*(1-2), pp. 227–246.

[22] Allaire, G., Jouve, F., and Toader, A.-M., 2004. "Structural optimization using sensitivity analysis and a level-set method". *Journal of computational physics, 194*(1), pp. 363–393.

[23] Kim, J., and Yoo, D.-J., 2020. "3d printed compact heat exchangers with mathematically defined core structures". *Journal of Computational Design and Engineering, 7*(4), pp. 527–550.

[24] Mirabolghasemi, A., Akbarzadeh, A., Rodrigue, D., and Therriault, D., 2019. "Thermal conductivity of architected cellular metamaterials". *Acta Materialia, 174*, pp. 61–80.

[25] Ye, Q., Guo, Y., Chen, S., Lei, N., and Gu, X. D., 2019. "Topology optimization of conformal structures on manifolds using extended level set methods (x-lsm) and conformal geometry theory". *Computer Methods in Applied Mechanics and Engineering, 344*, pp. 164–185.

[26] Gu, X. D., and Yau, S.-T., 2008. *Computational conformal geometry*, Vol. 1. International Press Somerville, MA.

[27] Lui, L. M., Gu, X., Chan, T. F., Yau, S.-T., et al., 2008. "Variational method on riemann surfaces using conformal

parameterization and its applications to image processing". *Methods and Applications of Analysis,* *15*(4), pp. 513–538.

[28] Lui, L. M., Wang, Y., and Chan, T. F., 2005. "Solving pdes on manifolds with global conformal parametriazation". In International Workshop on Variational, Geometric, and Level Set Methods in Computer Vision, Springer, pp. 307–319.

[29] Nguyen, T. H., Paulino, G. H., Song, J., and Le, C. H., 2010. "A computational paradigm for multiresolution topology optimization (mtop)". *Structural and Multidisciplinary Optimization,* *41*(4), pp. 525–539.

[30] Olver, P. J., 2017. "Complex analysis and conformal mapping". *University of Minnesota,* *806*.

[31] Osher, S., Fedkiw, R., and Piechor, K., 2004. "Level set methods and dynamic implicit surfaces". *Appl. Mech. Rev.,* *57*(3), pp. B15–B15.

[32] Choi, K. K., and Kim, N.-H., 2004. *Structural sensitivity analysis and optimization 1: linear systems*. Springer Science & Business Media.

[33] Allaire, G., 2015. "A review of adjoint methods for sensitivity analysis, uncertainty quantification and optimization in numerical codes". *Ingénieurs de l'Automobile,* *836*, pp. 33–36.

[34] Xia, Q., and Wang, M. Y., 2008. "Topology optimization of thermoelastic structures using level set method". *Computational Mechanics,* *42*(6), pp. 837–857.

[35] Al-Ketan, O., and Abu Al-Rub, R. K., 2019. "Multifunctional mechanical metamaterials based on triply periodic minimal surface lattices". *Advanced Engineering Materials,* *21*(10), p. 1900524.